Electronic Supplementary Material (ESI) for Inorganic Chemistry Frontiers.

Supporting Information

PtMn/PtCo Alloy Nanofascicles: Robust Electrocatalysts for Hydrogen Evolution Reaction under Both Acidic and Alkaline Conditions

Jinwu Hu, Caihong Fang, Xiaomin Jiang, Deliang Zhang, Zhiqing Cui

College of Chemistry and Materials Science, The Key Laboratory of Functional Molecular Solids, Ministry of Education, Anhui Laboratory of Molecular-Based Materials, Center for Nano Science and Technology, Key Laboratory of Electrochemical Clean Energy of Anhui Higher Education Institutes, Anhui Normal University, Wuhu, 241000, China

Characterization

Transmission electron microscopy (TEM) image was obtained using Hitachi HT7700 operating at an accelerating voltage of 120 kV. Scanning electron microscopy (SEM) and energy dispersive X-ray Spectroscopy (EDX) were operated on Hitachi 8100 scanning electron microscope. Elemental mapping was completed using Oxford. X-ray diffractometer (XRD) patterns come from SMART APEX Ⅱ. The XPS spectra were recorded on Escalab 250Xi. The absorption spectrum was collected on TU 1810. Inductively coupled plasma atomic emission spectroscopy (ICP-AES) was carried out using an Optima 300DV (PerkinElmer) to determine the composition of the alloy nanocrystals and mass of the electrocatalysts dropped on the working electrode.

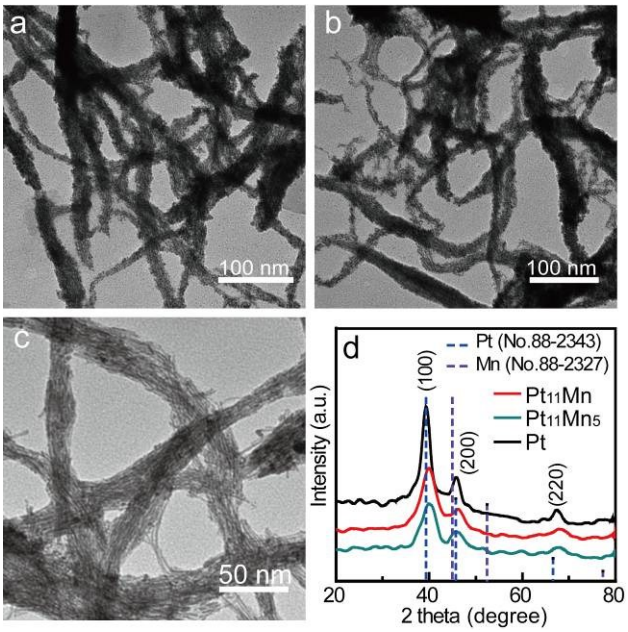

Fig. S1. (a−c) Representative TEM images of the Pt, $Pt_{11}Mn$ and $Pt_{11}Mn_5$ nanostructures, respectively. (d) XRD patterns of the Pt, $Pt_{11}Mn$ and $Pt_{11}Mn_5$ nanostructures.

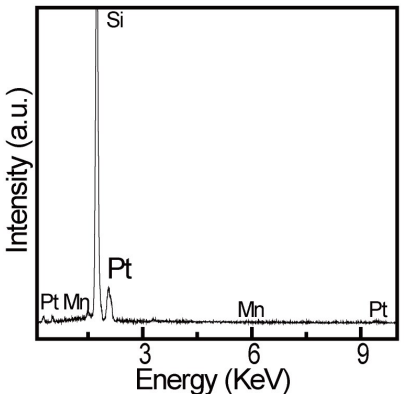

Fig. S2. EDX spectrum of Pt_6Mn NFs.

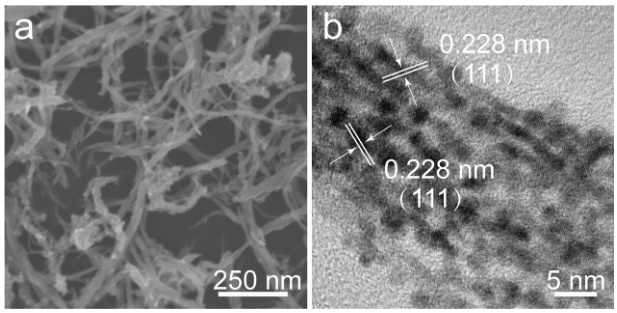

Fig. S3. Representative SEM (a) and HRTEM (b) of Pt_8Co FNFs, respectively.

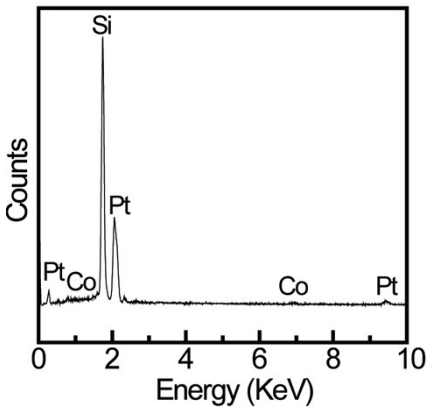

Fig. S4. EDX spectrum of Pt_8Co NFs.

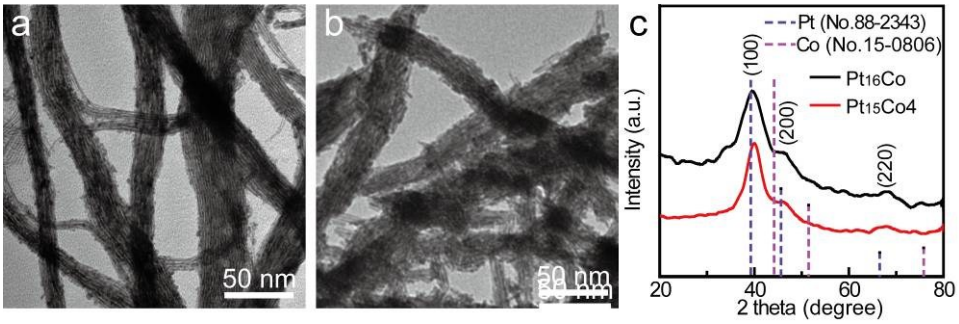

Fig. S5. (a,b) TEM images of $Pt_{16}Co$, and $Pt_{15}Co_4$ nanocrystals, respectively. (c) XRD pattern of the $Pt_{16}Co$, and $Pt_{15}Co_4$ nanocrystals.

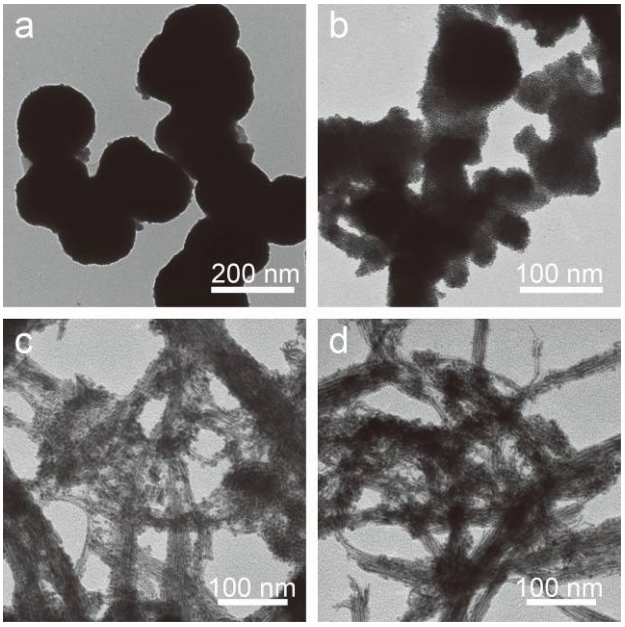

Fig. S6. TEM images of Pt_6Mn synthesized in varied amount of KOH of (a) 0 g, (b) 0.1 g, (c) 0.2 g, and (d) 0.3 g.

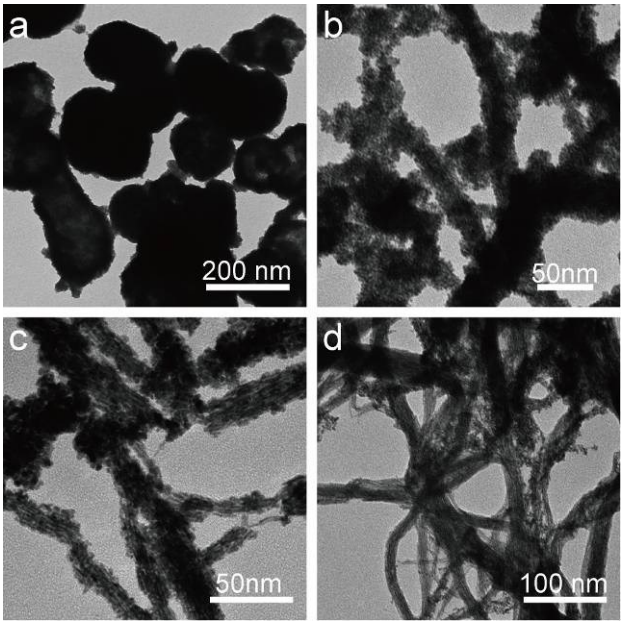

Fig. S7. TEM images of Pt_8Co with different amount of KOH of (a) 0 g, (b) 0.1 g, (c) 0.2 g, and (d) 0.3 g.

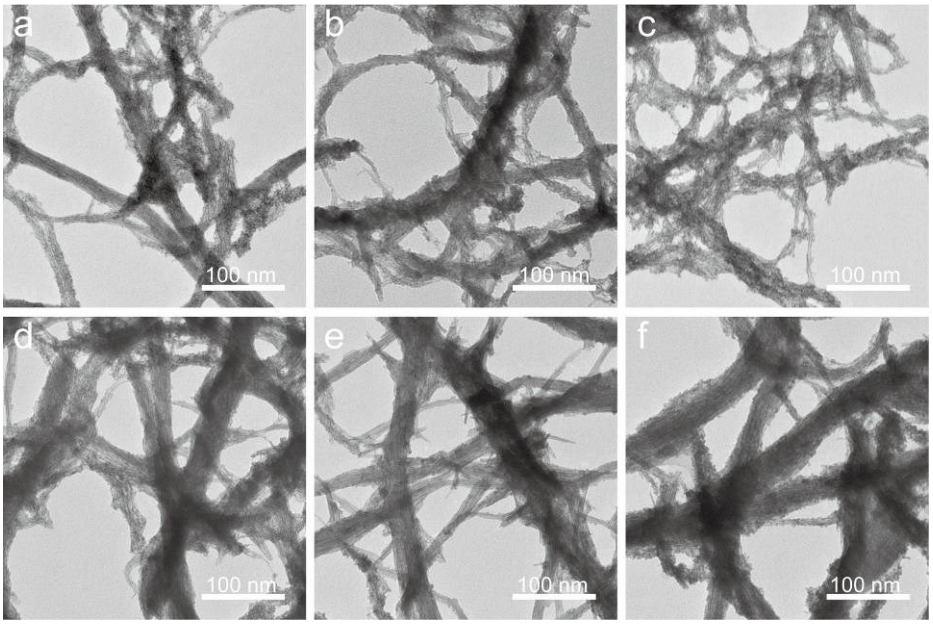

Fig. 8. (a−f) TEM images of PtCo alloy NFs synthesized with different reaction times of 10 min, 20 min, 30 min, 45 min, 1 h and 2 h, respectively.

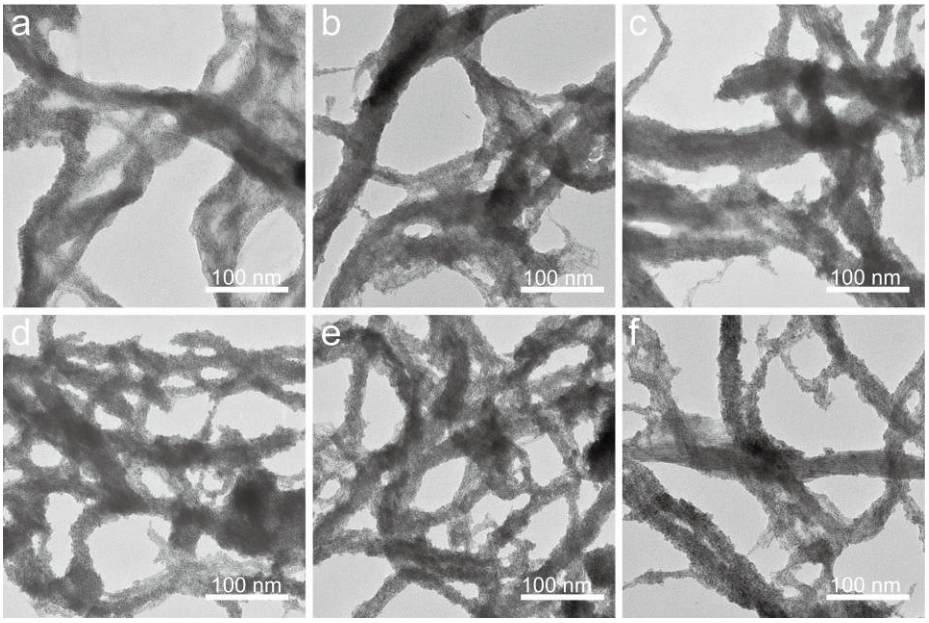

Fig. 9. (a−f) TEM images of PtMn alloy NFs synthesized with different reaction times of 10 min, 20 min, 30 min, 45 min, 1 h and 2 h, respectively.

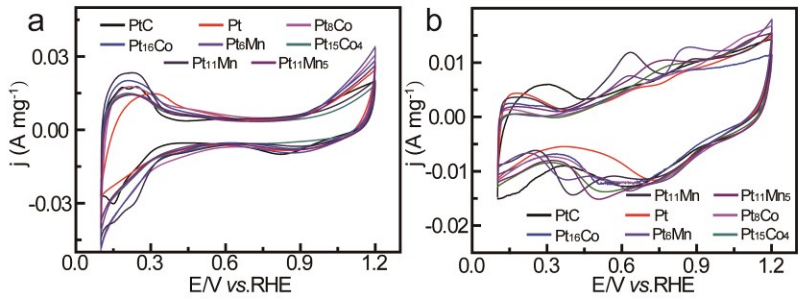

Fig. S10. (a,b) CV curves of $Pt_{16}Co$, Pt_8Co, $Pt_{15}Co_4$, $Pt_{11}Mn$, Pt_6Mn, $Pt_{11}Mn_5$ Pt, and commercial Pt/C in acid (H_2SO_4, 0.5 M) and alkaline solution (KOH, 1.0 M), respectively.

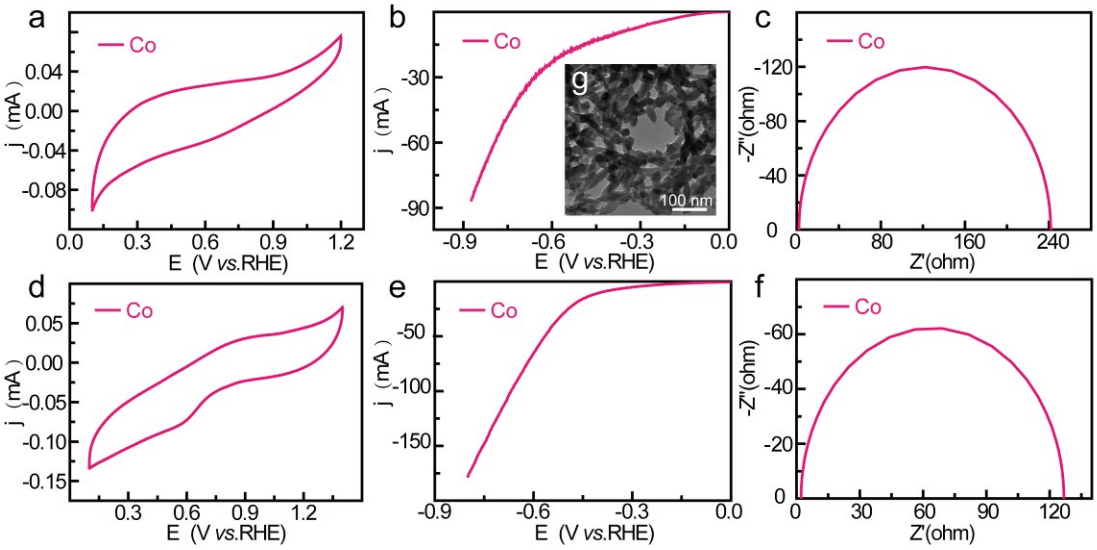

Fig. S11. CV curves, LSV polarization curves, and Nyquist plots of Co nanostructures measured in H_2SO_4 (0.5 M) (a−c), and KOH (1.0 M) (d−f), respectively.

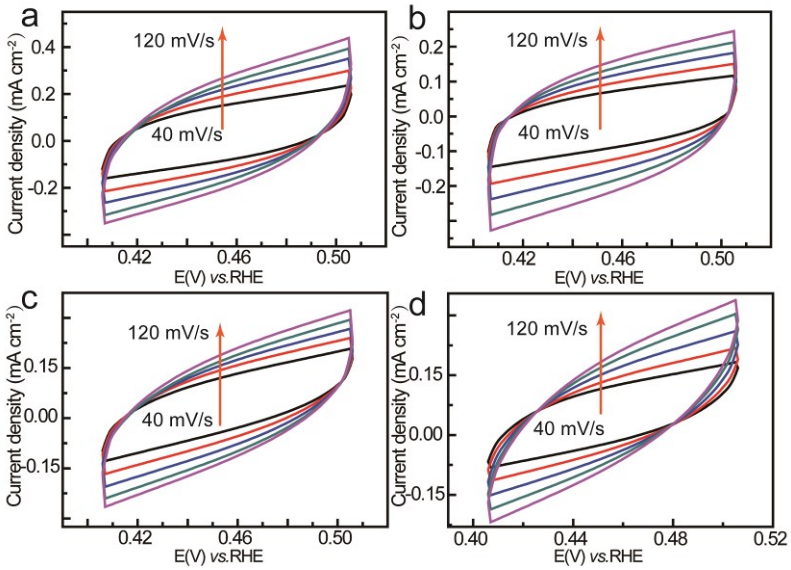

Fig. S12. (a−d) CV polarization curves of $Pt_{16}Co$, $Pt_{15}Co_4$, Pt, and commercial Pt/C in the nonfaradaic region with scan rates from 40 to 120 mV s^{-1} in H_2SO_4 (0.5 M), respectively.

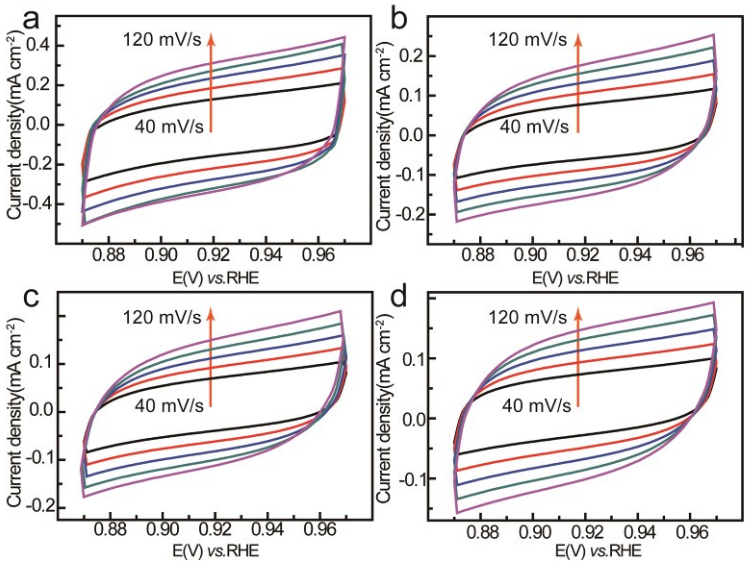

Fig. S13. (a−d) CV polarization curves of $Pt_{16}Co$, $Pt_{15}Co_4$, Pt and commercial Pt/C in the nonfaradaic region with scan rates from 40 to 120 mV s^{-1} in KOH (1.0 M), respectively.

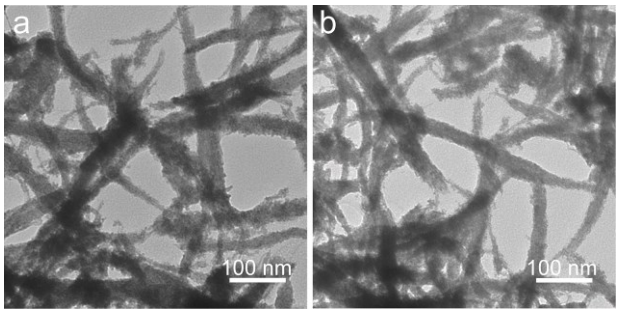

Fig. S14. (a,b) TEM images of the Pt_8Co electrocatalysts after CA tests in the acidic and alkaline condition, respectively.

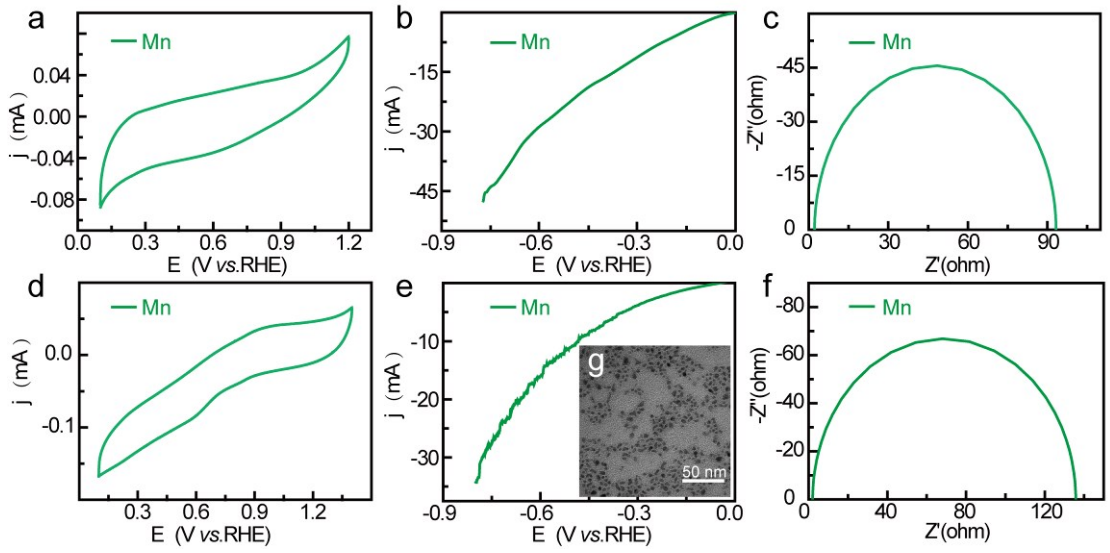

Fig. S15. CV curves, LSV polarization curves, and Nyquist plots of Mn nanocrystals in H_2SO_4 (0.5 M) (a−c), and KOH (1.0 M) (d−f), respectively.

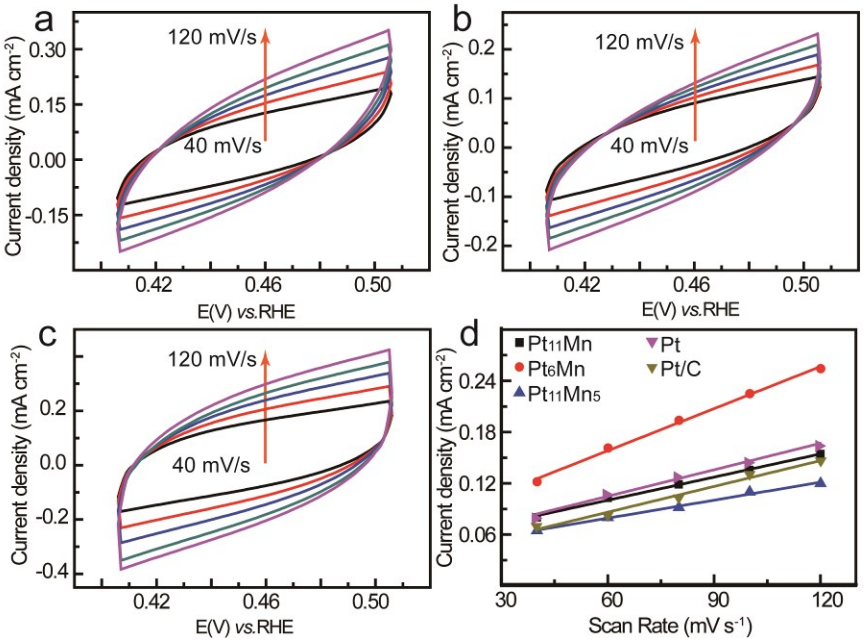

Fig. S16. (a−c) CV polarization curves of $Pt_{11}Mn$, $Pt_{11}Mn_5$, and Pt_6Mn NFs in the nonfaradaic region with scan rates from 40 to 120 mV s^{-1} in H_2SO_4 (0.5 M), respectively. (d) Double-layer capacitance (C_{dl}) plots of $Pt_{11}Mn$, Pt_6Mn, $Pt_{11}Mn_5$, Pt, and commercial Pt/C nanostructures in H_2SO_4 (0.5 M).

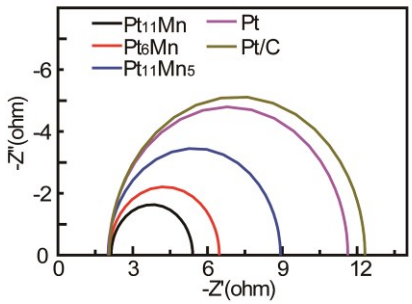

Fig. S17. Nyquist plots of $Pt_{11}Mn$, Pt_6Mn, $Pt_{11}Mn_5$, Pt and commercial Pt/C measured in H_2SO_4 (0.5 M).

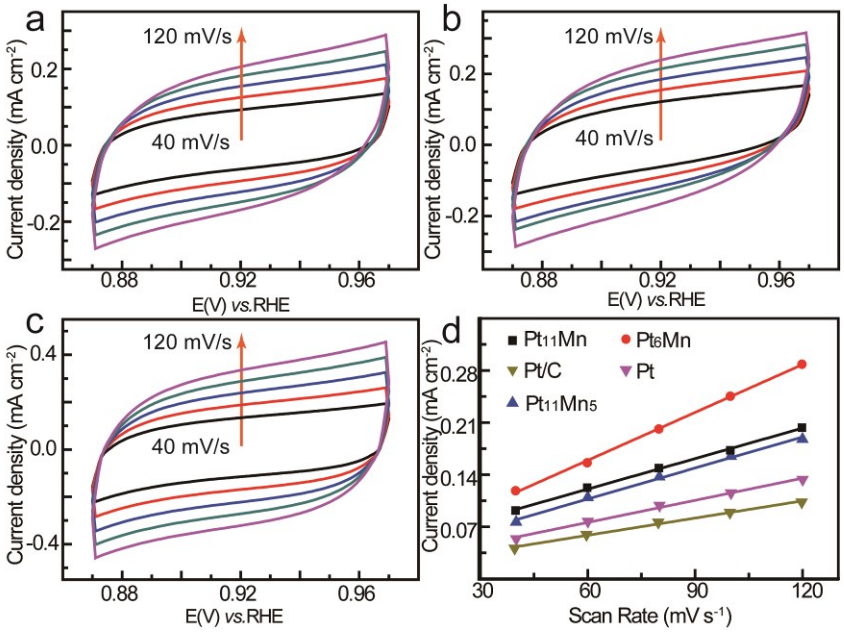

Fig. S18. (a−c) CV polarization curves of $Pt_{11}Mn$, $Pt_{11}Mn_5$, and Pt_6Mn in the nonfaradaic region with scan rates from 40 to 120 mV s^{-1} acquired in alkaline electrolyte (KOH, 1.0 M). (d) C_{dl} plots of $Pt_{11}Mn$, Pt_6Mn, $Pt_{11}Mn_5$, Pt nanocrystals, and commercial Pt/C in alkaline (KOH, 1.0 M).

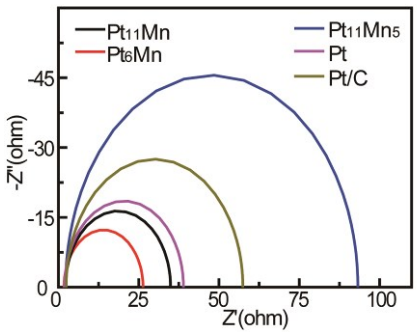

Fig. S19. Nyquist plots of $Pt_{11}Mn$, Pt_6Mn, $Pt_{11}Mn_5$, Pt and commercial Pt/C in KOH (1.0 M).

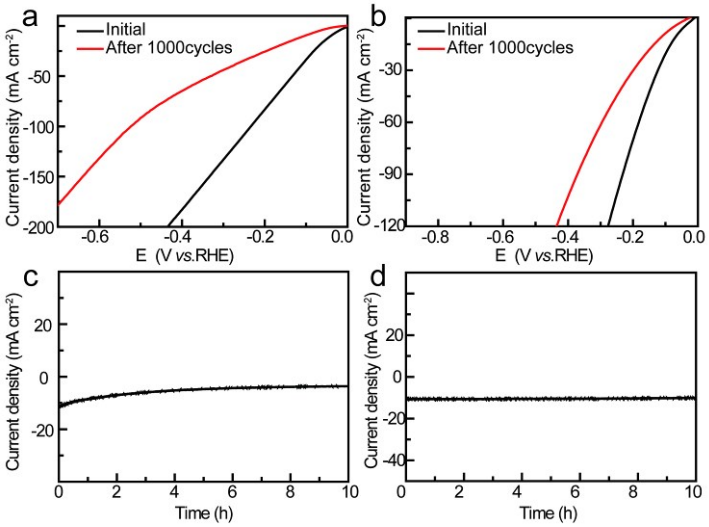

Fig. S20. (a,b) Durability test of Pt_6Mn electrocatalysts before and after1000 cycles in H_2SO_4 (0.5 M) and KOH (1.0 M), respectively. (c,d) CA curves of Pt_6Mn NFs in H_2SO_4 (0.5 M) and KOH (1.0 M) at a scan rate of 50 mV s^{-1}, respectively.

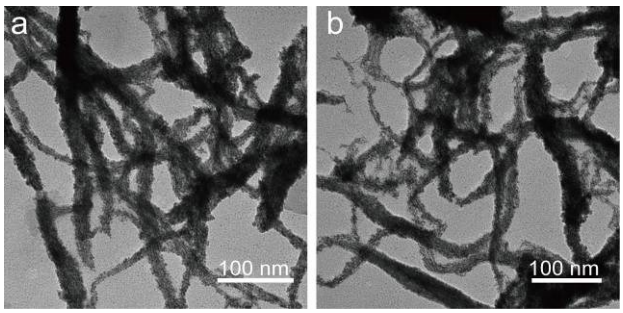

Fig. S21. (a,b)TEM images of the Pt_8Co electrocatalysts after CA tests in both the acidic and alkaline conditions, respectively.

Table S1. ICP-AES data of PtCo and PtMn nanostructures.

Catalyst	**Concentration (Pt)** (μg/L)	**Concentration (Co)** (μg/L)	**Concentration (Mn)** (μg/L)
$Pt_{16}Co$	31.7	1.97	
Pt_8Co	32	4.05	
$Pt_{15}Co_4$	31.1	8.3	
$Pt_{11}Mn$	30		2.92
Pt_6Mn	37.1		6.3
$Pt_{11}Mn_5$	36.5		16.35
Pt	35.5		
Co		8.9	
Mn			17.8

Table S2. ECSA of commercial Pt, Pt/C, $Pt_{16}Co$, Pt_8Co, $Pt_{15}Co_4$, $Pt_{11}Mn$, Pt_6Mn and $Pt_{11}Mn_5$ nanocrystals in both acid and alkaline solution.

Electrocatalyst	**ECSA ($m^2\ g^{-1}$) acid solution**	**ECSA ($m^2\ g^{-1}$) alkaline solution**
$Pt_{16}Co$	16.3	33.0
Pt_8Co	16.18	35.5
$Pt_{15}Co_4$	14.7	41.5
$Pt_{11}Mn$	17.1	29.1
Pt_6Mn	20.1	28.9
$Pt_{11}Mn_5$	19.3	37.2
Pt	18.1	31.3
Pt/C	21.3	33.7

Table S3. HER performances of commercial Pt/C, Pt, $Pt_{16}Co$, Pt_8Co, $Pt_{15}Co_4$, $Pt_{11}Mn$, Pt_6Mn, and $Pt_{11}Mn_5$ in acid solution.

Electrocatalyst	**Onset Potential (mV)**	**η_{10} (mV)**	**J_0 (mA cm^{-2})**	**Tafel slope (mV dec^{-1})**	**C_{dl} (mF cm^{-2})**
$Pt_{16}Co$	7.9	31.3	0.47	39	1.50
Pt_8Co	7.7	26.1	0.96	34	2.29
$Pt_{15}Co_4$	21.1	67.8	0.33	71	1.20
$Pt_{11}Mn$	12.3	41.7	0.69	48	0.925
Pt_6Mn	11.4	39.0	0.89	38	1.65
$Pt_{11}Mn_5$	19.8	67.9	0.35	56	0.701
Pt	13.3	49.8	0.451	43.1	1.059
Pt/C	15.7	63.4	0.23	58	0.97

Table S4. HER performances of commercial Pt/C, Pt, $Pt_{16}Co$, Pt_8Co, $Pt_{15}Co_4$, $Pt_{11}Mn$, Pt_6Mn and $Pt_{11}Mn_5$ in alkaline solution.

Electrocatalyst	**Onset Potential (mV)**	**η_{10} (mV)**	**J_0 (mA cm^{-2})**	**Tafel slope (mV dec^{-1})**	**C_{dl} (mF cm^{-2})**
$Pt_{16}Co$	27	67.1	0.43	56	2.35
Pt_8Co	12.9	47.2	1.096	50	3.30
$Pt_{15}Co_4$	32	97.1	0.27	67	1.20
$Pt_{11}Mn$	23.5	81.3	0.320	74	1.37
Pt_6Mn	26.3	67.5	0.627	54	2.45
$Pt_{11}Mn_5$	19.1	84	0.228	84	1.39
Pt	42	104.03	0.25	89	0.99
Pt/C	56	187.89	0.13	124	0.89